SSRG International Journal of Electrical and Electronics Engineering
ISSN: 2348-8379/ https://doi.org/10.14445/23488379/IJEEE-V11I7P119

Volume 11 Issue 7, 215-227, July 2024

Original Article

Forecasting Maximum Power Point in Solar Panels Using CNN-GRU

Diaa Salman[1], Yonis Khalif Elmi[2], Abdullahi Sheikh Mohamed[3], Yakub Hussein Mohamed[4]

[1,3,4]*Faculty of Engineering, Jamhuriya University of Science and Technology, Mogadishu, Somalia.*
[2] *Department of Electrical and Electronic Engineering, Cyprus International University, Nicosia, Northern Cyprus.*

[1]*Corresponding Author : D.salman@just.edu.so*

Received: 09 May 2024 Revised: 11 June 2024 Accepted: 09 July 2024 Published: 26 July 2024

Abstract *- The use of hybrid Convolutional Neural Network- Gated Recurrent Unit (CNN-GRU) models for solar panel Maximum Power Point (MPP) prediction is examined in this work. Improved solar energy forecasting accuracy is essential for grid integration and power-generating optimization. A novel CNN-GRU architecture that captures both temporal and spatial patterns present in solar energy data using a dataset that includes temperature, irradiance, and MPP characteristics is utilized. A comparison study with alternative hybrid architectures and individual GRU and CNN models. Model performance is evaluated by use of evaluation metrics such as coefficient of determination (R^2), Mean Squared Error (MSE), and Mean Absolute Error (MAE). Results show that the CNN-GRU model achieves better accuracy in forecasting voltage (Vmp) and current (Imp) at the MPP than individual architectures. Furthermore, residual analysis and prediction against actual comparisons prove the efficacy and robustness of the suggested method. The practical ramifications of this study for renewable energy management and grid stability advance solar energy forecasting methods.*

Keywords *- Solar energy forecasting, Maximum power point, Hybrid models, Predictive accuracy, Renewable energy optimization.*

1. Introduction

A recent fast advancement in solar PV energy technology has made it possible for the PV market to expand and lower material costs. Thus, it is essential to make technological advancements to keep the system operating steadily. A battery management system that is capable of efficiently managing the energy that is stored in the battery, as well as MPPT algorithms that are able to monitor the power, which improves real-time efficiency, are two examples of many techniques and modules used for developing the PV system.

Throughout the last ten years, photovoltaic systems have become the renewable technology with the quickest rate of growth and a crucial element of sustainable development. Though it has created much attention, the quick progress of photovoltaic power generation has also presented a problem [1].

The primary components of photovoltaic power generation include characteristics such as the intensity of solar irradiation, the temperature of the module and its surroundings, wind velocity, and other parameters that are based on meteorological conditions [2]. Photovoltaic power production will be intermittent and fluctuating if any minute changes take place, such as the instability or inconsistency of the subsequent dependency. Sudden disruptive occurrences could have serious repercussions for the grid-connected and stand-alone PV power system that would be hard to monitor and quantify [3]. Predicting accurately how much power a PV system will generate is crucial, and it has been noted as one of the main obstacles to extensive PV integration.

Solar forecasting basically gives the interested party—grid operators, for example—away. They would have to ensure that the production and consumption of energy are balanced in order to reduce expenses and attain competitiveness and economic viability. When the grid operator has a variety of generating assets at their disposal, accurate solar forecasting enables the operator to allocate their controllable units optimally.

In the event that a solar panel does not receive uniform irradiation, the circumstance that is known as partial shading may occur. A lot of different things could be the cause of this, including the presence of snow, passing clouds, surrounding buildings, towers, trees, and telephone poles. The PV panel's Power versus Voltage (P-V) curve is altered to have multiple peaks as a result of this condition, which causes the curve to have a convex appearance. This is because the PV panel is able to produce more power than it consumes [4].

In addition, it results in power losses and thermal stress on the photovoltaic panel at the same time. These adverse consequences are the result of the fact that specific photovoltaic cells within a photovoltaic panel become reverse-biased when exposed to partial shading conditions [5].

Traditional maximum power point tracking methods, which are intended to maximize the effectiveness of energy harvesting, are confronted with a challenge when confronted with the multi-peak power-voltage curve. It is unavoidable that a considerable amount of energy will be lost as a consequence of the fact that the present MPPT approaches are not designed to discover the global maximum power point. This, in turn, will result in a significant decrease in the efficiency of the PV system that is being considered. Furthermore, while they are in operation, these MPPT techniques usually find themselves confronted with issues such as sluggish convergence and power fluctuations in the steady state.

The challenges with maximum power point tracking that arise in scenarios involving partial shade have, in general, been addressed in two different ways. This is how these solutions are presented. Approaches that are hybridized with MPPT are included in the first category of various solutions. Combining the traditional MPPT algorithms with optimization and heuristic methods results in the creation of these techniques [6].

As part of the second category, unique MPPT strategies that are founded on heuristic methods are put forward for consideration. The approaches that fall under this category include, but are not limited to, simulated annealing [7], firefly algorithm [8], whale optimization [9], and team game optimization [10].

With regard to this particular domain, the Particle Swarm Optimization (PSO) maximum power point tracking method has shown an exceptional level of success in discovering the global maximum power point. However, this method has a slow tracking period, which leads to significant fluctuations and poor dynamic performance when the global maximum power point is being tracked [11].

This is because the monitoring period is slow. One of the potential options that was investigated was the utilization of the PSO in conjunction with other techniques, such as the perturb and observe approach, in order to cut down on the amount of time that was necessary for tracking [12].

Furthermore, certain modified PSO algorithms that implement some adjustments, such as adaptive parameters, were given [13]. This was done in order to improve the performance of the algorithm. Although these methods were designed to address certain PS situations, they still have a severe flaw, which is that they are unable to prevent becoming stuck in a local maximum power point. This is a significant limitation. It is feasible to come up with a more thorough solution. This can be accomplished by first gaining an understanding of the elements that lead to this behavior.

Because the PSO MPPT method is a dynamical system, its stability and steady-state assessments in the partial shading conditions demonstrate these causes and provide insight into how its performance can be improved even further. This is because the PSO MPPT algorithm is a dynamical system.

Because deep learning techniques may capture intricate non-linear correlations between solar power generation and related weather data, they have attracted special attention among forecasting techniques for solar generation [14].

Deep Neural Networks (DNNs) belonging to the Convolutional Neural Network (CNN) class can automatically learn and extract relevant features for a specific task without the requirement for human feature engineering or task comprehension in advance [15]. Although computer vision applications were the original purpose for these networks, solar power forecasting has shown promise in recent years [15].

As the population and industries seek cleaner solutions, sunlight has become an essential component of the electricity generated and utilized all over the world; for this, it is required to ensure forecasting of the maximum power point in the solar panels. Nevertheless, this task is complex due to fluctuations in the surroundings, such as temperature and irradiance.

The previous literature has mainly considered the usage of RNNs such as GRU or CNNs for this task. At the same time, few have investigated the application of the combined form of both architectures. However, there is no extensive comparison of the experiments to choose the best model architecture for the given application.

This study aims to fill the above research gap with a clear objective of comparing and evaluating the performance of the chosen models, including GRU, CNN, GRU-CNN, and CNN-GRU, in the task of MPP forecasting for solar panels. These hybrid models are expected to outperform the others because of the temporal dependencies obtained from the GRU mechanism and the spatial features extracted from the CNN. The primary goal is to find the best topology for forecasting the voltage and current at MPP to improve the photovoltaic system's performance.

This work compares and combines several unique advanced machine learning models, including GRU, CNN, GRU-CNN, and CNN-GRU, which is a fresh approach different from other related works. The goal is to determine where solar panels will generate the most incredible power.

An extensive study of a range of uses has been done on individual models, including CNN and GRU. Conversely, the combination of both models in GRU-CNN and CNN-GRU designs offers a unique approach to maximize the advantages connected with both recurrent and convolutional neural networks. This hybridization aims to improve the accuracy of predictions by combining the temporal dependencies and the spatial characteristics of the input data (Temperature and Irradiance).

2. Problem Identification

2.1. Models Overview

Forecast solar electricity. This comparison takes into account the topologies of each model in addition to the assessment criteria that are associated with each model. Seven research studies are compared and contrasted in Table 1. These studies focus on different kinds of models, datasets, assessment measures, and notable discoveries.

Researchers from all over the world carried out these investigations. Additionally, the structures of the GRU, CNN, and hybrid CNN-GRU models are depicted in Figures 1 through 3, respectively. These figures display the architectures of the models [16, 17].

The main contribution of this work can be stated in the innovative approach to the models' creation, which is based on the CNN and GRU deep learning networks that enhance the accuracy of solar power forecasting. The prior studies, for instance, Amreen et al. (2023) [18], are more concerned with employing GRU for hour-ahead, which demonstrates promising gains against conventional approaches.

However, other researchers figured out that LSTM and CNN models can be used individually, as reviewed in a study carried out at Visvesvaraya National Institute of Technology (VNIT), Nagpur that applied LSTM, CNN, and Linear Regression (LR) models for forecasting of solar power for educational buildings. In this study, LSTM was established to be the fit model and was more accurate than CNN and LR.

The study contributes to this area by combining the superiority of both CNN and GRU structures for a more accurate prediction of values. The CNN part learns spatial patterns from the input data, and the GRU layers learn temporal patterns, which are also more robust and comprehensive.

The above experiments have also shown that this combined model outperforms the completely separate GRU and CNN models with the same inputs through the values of MAE and MSE. Therefore, eliminating the drawbacks of the approaches used and offering an efficient solution to improve the accuracy of the sun power forecast, this work enhances further investigations to enhance the efficiency of managing and repairing solar power plants.

Using cutting-edge machine learning techniques, there have been major efforts made to enhance the accuracy of PV power forecasting, as can be seen from the review of the relevant literature. The authors such as Qing et al. (2022) proposed a novel multi-step ahead PV power forecasting model that includes data augmentation by TimeGAN, soft DTW-K-medoids clustering for extracting time series features, and a CNN-GRU hybrid neural network. This model was developed in order to forecast PV power in the future [19].

Their model proved to have a better accuracy in predicting the weather conditions compared to the conventional methods as depicted by their model. In the same vein, For PV power forecasting, Abdellatif et al. (2024) examined the performance of three different models: the Bidirectional Long Short-Term Memory (Bi-LSTM), the 1D-CNN, and the GRU. This was done mainly during the day and during the night [20].

According to their findings, all the models they used had high accuracy, but Bi-LSTM and GRU surpassed 1D-CNN, especially in cases involving night-time data. Amit et al. (2023) proposed a new model, a differential attention-based model with CNN and BiLSTM as two parallel branches, with an attention mechanism for learning long-term dependencies and Bayesian optimization for hyperparameters tuning [21].

They demonstrated significant enhancements in the predictive accuracy of their model when compared with the datasets originating from different regions. Altogether, these works collectively illustrate the constant improvement of PV power forecasting and the effectiveness of the hybrid and attention-based models in reaching higher accuracy and reliability in forecasting.

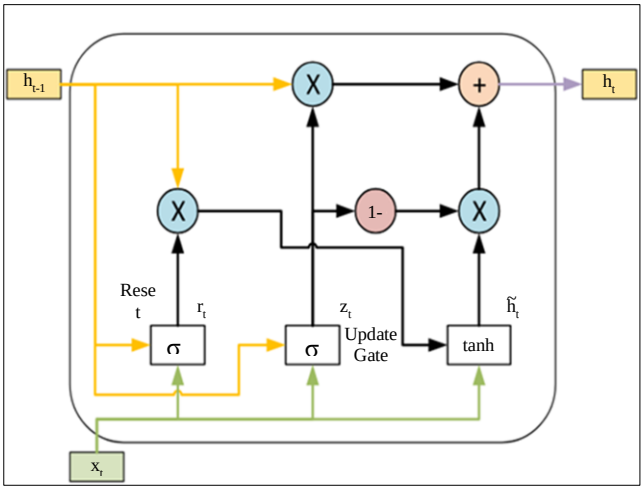

Fig. 1 Architecture of GRU model [26]

Table 1. Comparison of studies on solar power forecasting models

Reference	Model Type	Dataset Description	Evaluation Metrics	Main Findings
[19]	Hybrid CNN-GRU	Data from two 50 MW PV power stations in Xinjiang, China.	RMSE, MAE, R^2	The CNN-GRU model achieved superior accuracy, with lower RMSE values for both sunny and cloudy days.
[22]	Hybrid GRU and XGBoost	Historical solar energy and NWP data from Tianchi UNiLAB and GEFCom2014.	MSE, MAE	The GRU-XGBoost model significantly reduced MSE and MAE, outperforming other models.
[23]	Various DL techniques, including CNN, GRU, LSTM	Industrial PV plant datasets from various locations.	RMSE, MAE, MAPE	Hybrid DL models, especially CNN-GRU, showed higher accuracy than stand-alone models.
[20]	Bi-LSTM, GRU, 1D-CNN	207,088 samples from a rooftop PV system in Morocco.	R^2, MAE, MSE, RMSE, ME	Bi-LSTM, GRU, and 1D-CNN models provided high prediction accuracy, particularly in sunny conditions.
[21]	Hybrid CNN-BiLSTM with Attention	Real-time solar plant data from Australia and India.	MSE, MAE	The differential attention net improved MSE and effectively captured temporal dependencies.
[24]	LSTM, BiLSTM, GRU, BiGRU, CNN1D, CNN1D-LSTM, CNN1D-GRU	Data from a PV microgrid at the University of Trieste.	RMSE, MAE, MAPE, r	LSTM and GRU models provided the best results, with high correlation coefficients.
[25]	Hybrid WPD-LSTM	Data from a PV system in Alice Springs, Australia.	MBE, MAPE, RMSE	The WPD-LSTM model outperformed other models, showing lower error values across different conditions.

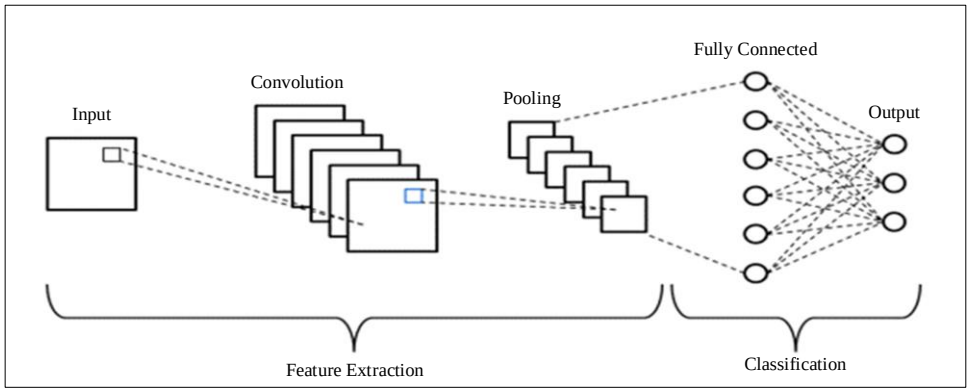

Fig. 2 Architecture of CNN model [27]

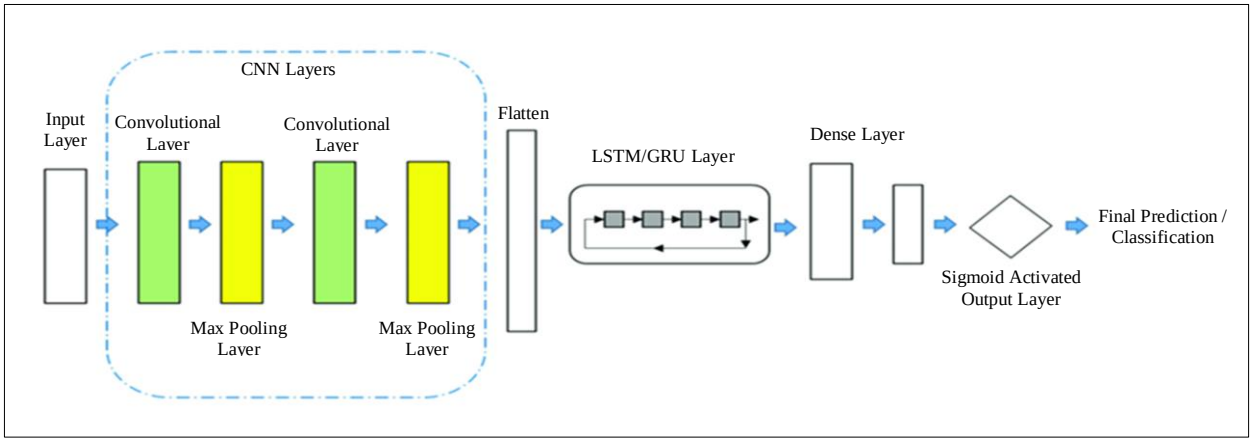

Fig. 3 Architecture of hybrid CNN-GRU model [28]

2.2. Mathematical Formulations of GRU and CNN Models

2.2.1. GRU Model Formulation

One particular type of Recurrent Neural Network (RNN) is known as the Gated Recurrent Unit (GRU), which was designed specifically to identify correlations in sequential input sources. There are a great number of different types of RNNs as well; this particular one is one among them [29]. GRUs consist of gating units that modulate the flow of information inside the unit, as described by the following equations.

$$z_t = \sigma\left(\sum_{i=1}^{n} W_{zi} x_{ti} + \sum_{j=1}^{m} U_{zj} h_{(t-1),j} + b_z\right) \quad (1)$$

$$r_t = \sigma\left(\sum_{i=1}^{n} W_{ri} x_{ti} + \sum_{j=1}^{m} U_{rj} h_{(t-1),j} + b_r\right) \quad (2)$$

$$\tilde{h}_t = \tanh\left(\sum_{i=1}^{n} W_{hi} x_{ti} + r_t * \left(\sum_{j=1}^{m} U_{hj} h_{(t-1),j}\right) + b_h\right) \quad (3)$$

$$h_t = (1 - z_t) * h_{(t-1)} + z_t * \tilde{h}_t \quad (4)$$

Where,

- z_t is the update gate at time step t, controlling how much of the past state $h_{(t-1)}$ is used.
- r_t is the reset gate at time step t, determining how much of the past state to forget.
- $\tilde{h}_t$ is the candidate activation, a combination of the current input x_t and the modulated past state.
- h_t is the final hidden state at time step t .
- σ is the sigmoid activation function.
- tanh is the hyperbolic tangent activation function.
- W_{zi}, W_{ri} , and $W_{hi}$are weight matrices for the input features.
- U_{zj}, U_{rj}, and U_{hj} are weight matrices for the hidden states.
- b_z, b_r, and $b_h$are biased terms.

These equations enable the GRU to capture temporal dependencies effectively in sequential data. As illustrated in Equation 1, the update gate z_t incorporates the current input and the previous hidden state, allowing the model to decide how much past information to retain.

Equation 2 demonstrates the reset gate r_t, which facilitates the forgetting mechanism by selectively resetting parts of the past hidden state. Equation 3 elaborates on the candidate activation $\tilde{h}_t$, combining current inputs and modulated past states to form a candidate for the new hidden state.

Lastly, Equation 4 shows the GRU output h_t, merging the retained past information with the candidate activation to produce the final hidden state for the current time step [30].

2.2.2. CNN Model Formulation

Convolutional Neural Networks (CNNs) are designed to process data with a grid-like topology, such as time-series data or image data. The critical components of a CNN include convolutional layers and pooling layers. The equations governing these layers are described below.

Convolutional Layer Equation

$$Y_{i,j,k} = \sum_{m=0}^{M-1} \sum_{n=0}^{N-1} \sum_{c=0}^{c-1} x_{i+m,j+n,c} \cdot W_{m,n,c,k} + b_k \quad (5)$$

Pooling Layer Equation

$$Z_{i,j,k} = \max_{0 \leq m < P, 0 \leq n < Q} Y_{pi+m,qj+n,k} \quad (6)$$

Where,

- $Y_{i,j,k}$ is the output feature map at position (i, j) for the (K-th) filter.
- $x_{i+m,j+n,c}$ is the input data at position $(i + m, j + n)$ for channel c .
- $W_{m,n,c,k}$ is the weight of the filter at position $m, n)$for channel c and filter k.
- b_k is the bias term for the (K-th) filter.
- $Z_{i,j,k}$ is the output of the pooling layer at position (i, j) for the (K-th) feature map.
- max denotes the max-pooling operation, which selects the maximum value within the pooling window.

The convolutional layer is responsible for computing the output feature map, as demonstrated in Equation 5. This is accomplished by applying a set of filters to the input data, which then effectively captures local patterns.

As shown in Equation 6, the pooling layer is responsible for reducing the spatial dimensions of the feature maps. This allows for the retention of only the most significant characteristics while also improving computational efficiency. [31].

3. Methodology

3.1. Establishing the CNN-GRU Model

In this part, the CNN-GRU model's design and setup for solar panel maximum power point predictions are described and illustrated in Figure 4.

3.1.1. Input Layer

First in the model is an input layer made to manage sequential data. More significantly, the features employed in prediction, such as the values of temperature and irradiance, are reflected in the input shape. The input data structure allows for the time-series character of the problem, which qualifies it for additional processing by the CNN and GRU levels.

3.1.2. Layers of A Convolutional Neural Network (CNN)

Convolutional Neural Networks (CNNs) are used by the first component of the model to extract spatial information from the input data. Local dependencies and patterns in the data are captured in significant part by the CNN layers. Comprising this arrangement are:

- The First Convolutional Layer: Uses several filters to carry out convolution procedures along the input stream. Non-linearity brought about by the ReLU activation function improves the model's capacity to grasp intricate patterns. Batch normalization is the application of normalizing the convolutional layer output to stabilize and speed up the training process.
- Layer 2 Convolutional: Further processing of the features obtained by the first layer is done by another convolutional layer. Using a bigger kernel size captures wider patterns. It ensures stability and efficiency throughout training by using batch normalization and ReLU activation, the same as the first layer.
- Layers of Flattening: The multi-dimensional feature maps are flattened to produce a one-dimensional vector as the output of the CNN layers. This stage makes the data consistent with the input requirements of the GRU layers that follow, therefore preparing it for them.

3.1.3. Reshape Layer

The data is then reformed to have the proper size that the GRU layers need once it has been flattened. Maintaining the sequential character of the input, this reshaping is essential since it converts the data into a format that the GRU layers can handle efficiently.

3.1.4. Layers of the Gated Recurrent Unit (GRU)

The model captures temporal dependencies in the data using several GRU layers. Particularly well-suited for sequential data, GRUs perform well at time-series forecasting. Setup comprises:

- First Layer of GRU: The many units in this layer process the altered data and generate return sequences. Through the capacity to return sequences, the model is able to record temporal dependencies over several time steps and process the input further by later GRU layers.
- Extra GRU Layers: Complex temporal relationships are captured even more by the data processing of further GRU layers. These layers improve the capacity of the model to understand the sequence information included in the data, therefore generating more accurate forecasts.

3.1.5. Dropout Layers

A dropout layer has been included to help lower overfit and enhance model generalization. This layer generates a random drop of a given proportion of the units during the training process, which drives the model to acquire more robust properties that are less sensitive to particular training samples.

Layer (type)	Output Shape	Param #	Connected to
input_2 (InputLayer)	[(None, 1, 2)]	0	[]
conv1d_2 (Conv1D)	(None, 1, 64)	448	['input_2[0][0]']
batch_normalization_2 (BatchNormalization)	(None, 1, 64)	256	['conv1d_2[0][0]']
conv1d_3 (Conv1D)	(None, 1, 64)	20544	['batch_normalization_2[0][0]']
batch_normalization_3 (BatchNormalization)	(None, 1, 64)	256	['conv1d_3[0][0]']
flatten_1 (Flatten)	(None, 64)	0	['batch_normalization_3[0][0]']
reshape (Reshape)	(None, 1, 64)	0	['flatten_1[0][0]']
gru (GRU)	(None, 1, 64)	24960	['reshape[0][0]']
gru_1 (GRU)	(None, 1, 64)	24960	['gru[0][0]']
gru_2 (GRU)	(None, 1, 64)	24960	['gru_1[0][0]']
dropout (Dropout)	(None, 1, 64)	0	['gru_2[0][0]']
flatten_2 (Flatten)	(None, 64)	0	['dropout[0][0]']
dense (Dense)	(None, 128)	8320	['flatten_2[0][0]']
dense_2 (Dense)	(None, 128)	8320	['flatten_2[0][0]']
dropout_1 (Dropout)	(None, 128)	0	['dense[0][0]']
dropout_2 (Dropout)	(None, 128)	0	['dense_2[0][0]']
dense_1 (Dense)	(None, 64)	8256	['dropout_1[0][0]']
dense_3 (Dense)	(None, 64)	8256	['dropout_2[0][0]']
Vmp (Dense)	(None, 1)	65	['dense_1[0][0]']
I_mp (Dense)	(None, 1)	65	['dense_3[0][0]']

Total params: 129666 (506.51 KB)
Trainable params: 129410 (505.51 KB)
Non-trainable params: 256 (1.00 KB)

Fig. 4 Hybrid CNN-GRU model architectur

3.1.6. Dense Layers

The last element of the model, which generates output forecasts, are very dense layers. Together, these layers make up the last component; inside, there are several layers:

- Many deep layers, including ReLU activation functions, are generated once the GRU layers have been processed. Dense layers with drop out are the layers that show drop off. Dropout is also carried out to these deep layers in order to prevent overfitting and ensure that the model generalizes well to data not observed. This is carried out to guarantee the accuracy of the model.
- Generation of the forecasts of the MPP (Vmp) and the current at MPP (Imp) depends on the last thick layers, sometimes referred to as the output layers. The output layers compute these forecasts. Every output layer is designed expressly to produce accurate projections for the goals that match it. The traits and patterns found by the layers before it help one to derive these projections.

Dropout and thick layers, CNN and GRU layers, and other layers taken together produce an all-encompassing model. This approach can effectively include temporal and spatial dependencies in the data. Regarding the performance of solar panels, this model can generate reliable and consistent forecasts.

3.2. Data Description

The dataset that was utilized for this investigation is comprised of four primary components. Temperature, irradiation, voltage at maximum power point (Vmp), and current at maximum power point (Imp) are some of the variables that are being discussed in this context.

As illustrated in Figure 5, temperature and irradiance are depicted as heatmaps, and each variable is represented in a matrix fashion. The correlation coefficients between variables are shown on the heatmaps; a perfect positive correlation is indicated by a value of 1.00, a perfect negative correlation of -1.00, and no correlation of 0.00.

Remarkably, a 0.28 correlation between temperature and irradiance is found, indicating a relatively positive association between both environmental variables.Moreover, while the correlation between Irradiance and Vmp is 0.29, indicating a slightly stronger positive association, the correlation between the temperature and Imp is recorded as -0.019, suggesting a faint negative link.

Similar connections between Imp and Imp, irradiance and Imp, and temperature and Vmp are also shown. Important new information on the interrelationships among the factors important for solar energy forecasting is provided by this data description [32].

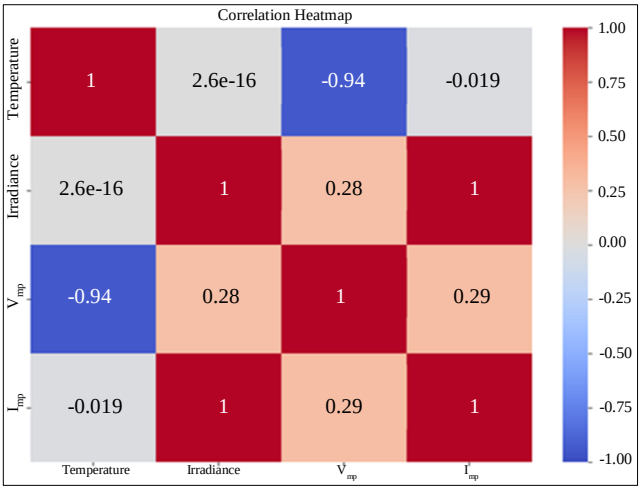

Fig. 5 The correlation matrix of the data

3.3. The Workflow of the Study

The work is divided into multiple critical phases to guarantee an accurate and systematic approach to employing powerful machine learning models to forecast the highest power point in solar panels, as illustrated in Figure 6 and in the following steps:

Step 1 : Preprocessing and cleaning of the data starting with the dataset preparation for analysis is the first step. This covers managing missing values, standardizing the data, and making sure every feature is formatted correctly for model input. Increased accuracy and efficiency of the machine learning models depend on appropriate data cleaning and preparation.

Step 2 : Model selection, where several machine learning architectures are used to find the best model for the forecasting problem. Considered models are Convolutional Neural Network (CNN), Gated Recurrent Unit (GRU), CNN-CNN (a hybrid of GRU and CNN), and CNN-GRU (another hybrid architecture with a different layer sequence). The choice of the most effective method depends on this procedure since every model has particular benefits in terms of gathering various sections of the data. This is so as every model offers certain benefits.

Step 3 : Following the completion of the cleaning and preprocessing of the dataset, the next step is to build training and testing subsets of the dataset. The training set is used to instruct the models, while the testing set is used to evaluate how well they perform. In order to determine the extent to which the models can be generalized, it is required to divide them.

Step 4 : Training and testing of the models: The training dataset is used to train each chosen model. The models pick up mapping the input properties (temperature and irradiance) to the output targets (Vmp and Imp) during this stage. The models are

evaluated for their predictive power on the testing dataset following training. The optimal performance of the models is achieved by fine-tuning their hyperparameters in this stage.

Step 5 : The trained models are assessed using a number of performance indicators, such as the coefficient of determination (R^2), Mean Absolute Error (MAE), and Mean Squared Error (MSE). The quantitative evaluation of the accuracy of each model in forecasting the highest power point in solar panels is given by these criteria.

Step 6 : The model with the most fantastic accuracy and generalization ability is chosen as the best model based on the performance evaluation. The best model is identified as the investigation comes to an end if its performance satisfies the required standards. In the absence of such, the process loops back to the model selection stage to reevaluate and maybe modify the model selection procedure, guaranteeing ongoing enhancement and optimization of the forecasting model.

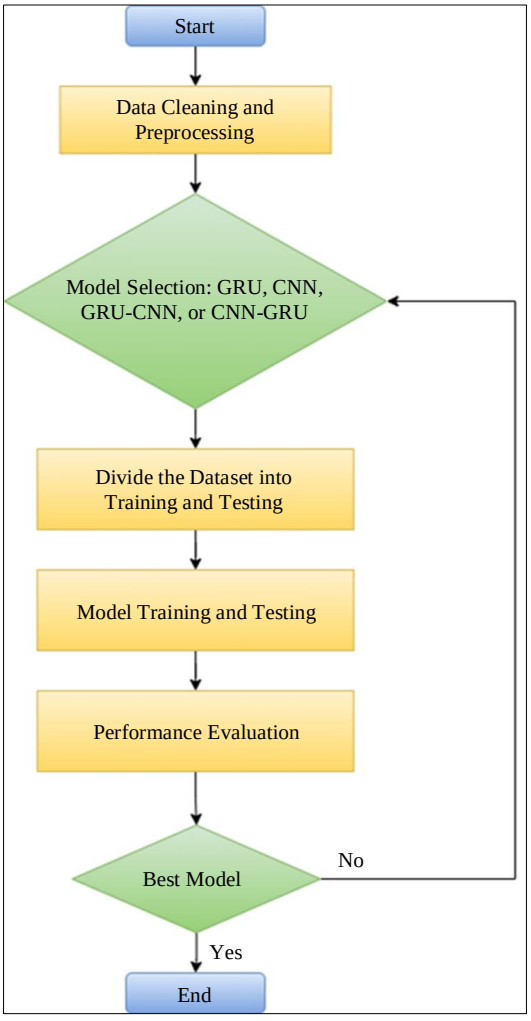

Fig. 6 The workflow and model selection flowchart

4. Results and Discussion

4.1. Performance Evaluation

The performance metrics for the four models; GRU, CNN, GRU-CNN, and CNN-GRU-in forecasting the maximum power point parameters; Vmp (Voltage at Maximum Power Point) and Imp (Current at Maximum Power Point) are thoroughly compared in Table 2. Metrics assessed include the coefficient of determination (R^3), Mean Squared Error (MSE), and Mean Absolute Error (MAE).

At an MAE of 0.08651, an MSE of 0.0379, and a R^2 of 0.98664 for Vmp, the GRU model performs really well. It accomplishes for Imp an R^2 of 0.99401, an MSE of 0.0288, and an MAE of 0.13421. Though it does well overall, especially in terms of R^2 for Imp, the GRU model does not outperform the other models.

By contrast, the CNN model has an R^2 of 0.98055, a higher MAE of 0.15108, and an MSE of 0.0552 for Vmp. It obtains for Imp an R^2 of 0.99551, an MSE of 0.0216, and an MAE of 0.10899. Although the CNN model predicts Imp somewhat better than Vmp, generally, its accuracy for Vmp is not higher than that of the GRU model.

At an MAE of 0.09090, an MSE of 0.0326, and a R^2 of 0.98851 for Vmp, the hybrid GRU-CNN model shows better performance. With an MAE of 0.07018, an MSE of 0.0081, and an R^2 of 0.99831, this model much beats the prior ones for Imp. These findings imply that improved overall performance can be obtained by merging GRU and CNN layers to catch more intricate patterns in the data.

Lastly, albeit having a somewhat higher MSE for Imp at 0.0504, the CNN-GRU model performs the best for Imp prediction with an MAE of 0.05042. Its greatest R^2 of 0.99912 for Imp indicates a perfect fit. It records for Vmp an R^2 of 0.98631, an MSE of 0.0389, and an MAE of 0.07130. The CNN-GRU model yields competitive results even though its MSE for Vmp is lower than that of the GRU-CNN model.

In conclusion, the resilient choice is the GRU-CNN model, which provides a balanced performance with low MAE and MSE and high R^2 values for both Vmp and Imp. But, since the CNN-GRU model predicts Imp so well, it seems to be better at capturing the current-related patterns. These results emphasize the advantages of hybrid models in solar energy forecasting applications that take advantage of both GRU and CNN architectures.

Figure 7, showing the relationship between Loss and Epoch for the various models across 1000 epochs, offers important information about their training characteristics. Effective learning and convergence are indicated by the GRU model's constant loss drop in Figure 7(a), which is consistent with its comparatively low MAE and MSE for both Vmp and Imp.

Table 2. A comparison between the model's performances

Model		MAE	MSE	R^2
GRU	Vmp	0.08651	0.0379	0.98664
	Imp	0.13421	0.0288	0.99401
CNN	Vmp	0.15108	0.0552	0.98055
	Imp	0.10899	0.0216	0.99551
GRU-CNN	Vmp	0.09090	0.0326	0.98851
	Imp	0.07018	0.0081	0.99831
CNN-GRU	Vmp	0.07130	0.0389	0.98631
	Imp	0.05042	0.0504	0.99912

Given its greater MAE and MSE for Vmp, which may not adequately capture temporal dynamics-Figure 7(b) displays the CNN model with a comparable but less noticeable loss. Drawing on the temporal sequence management of the GRU and the pattern recognition capabilities of the CNN, Figure 7(c) shows a more noticeable reduction in loss. Higher R^2 values and reduced MAE and MSE for this hybrid model, especially for Imp, indicate improved predictive accuracy. Finally, Figure 7(d) for the CNN-GRU model combines the advantages of both architectures for efficient sequence learning and feature extraction with an early fast loss reduction followed by a slow fall. This model performs remarkably well in current prediction, as seen by its lowest MAE and greatest R^2 for Imp. Both hybrid models outperform the individual GRU and CNN models overall; the CNN-GRU model excels in Imp prediction, demonstrating the benefits of combining convolutional and recurrent layers for precise solar energy forecasting, while the GRU-CNN model achieves the best balance for Vmp and Imp predictions.

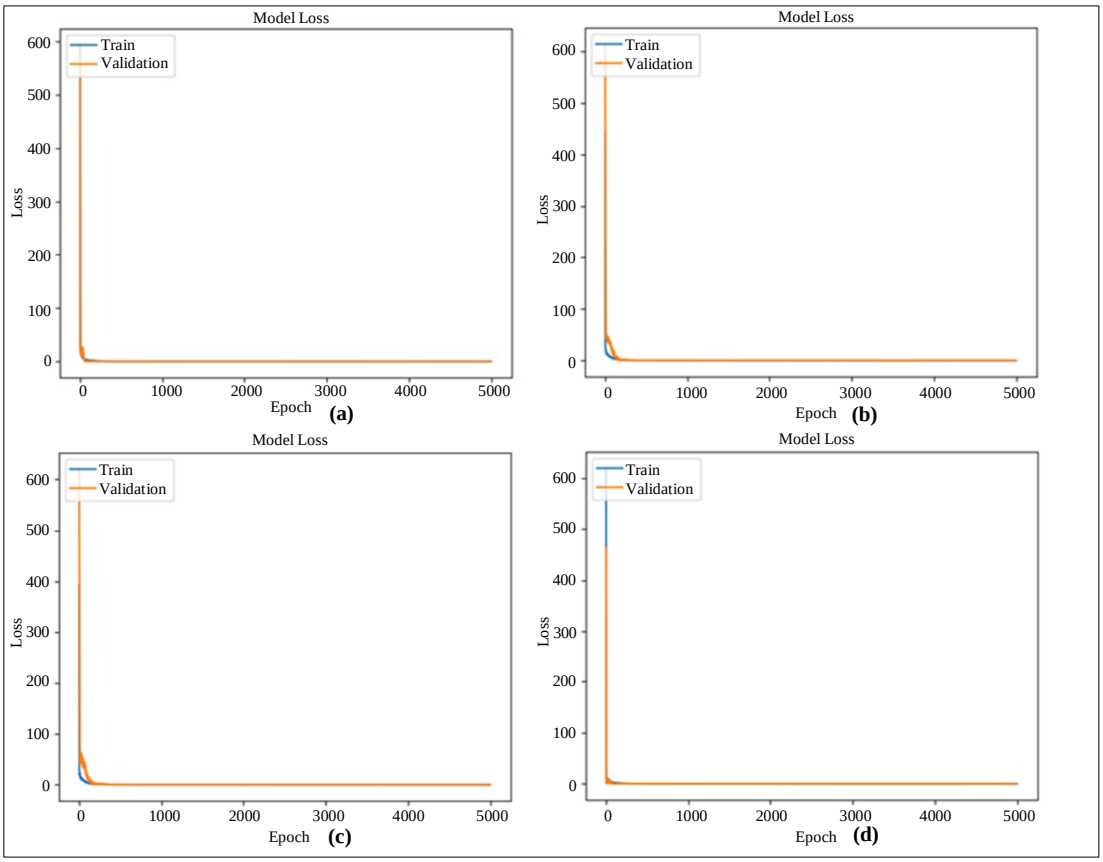

Fig. 7 Comparison of model loss across epochs for (a) GRU, (b) CNN, (c) GRU-CNN, and (d) CNN-GRU architectures.

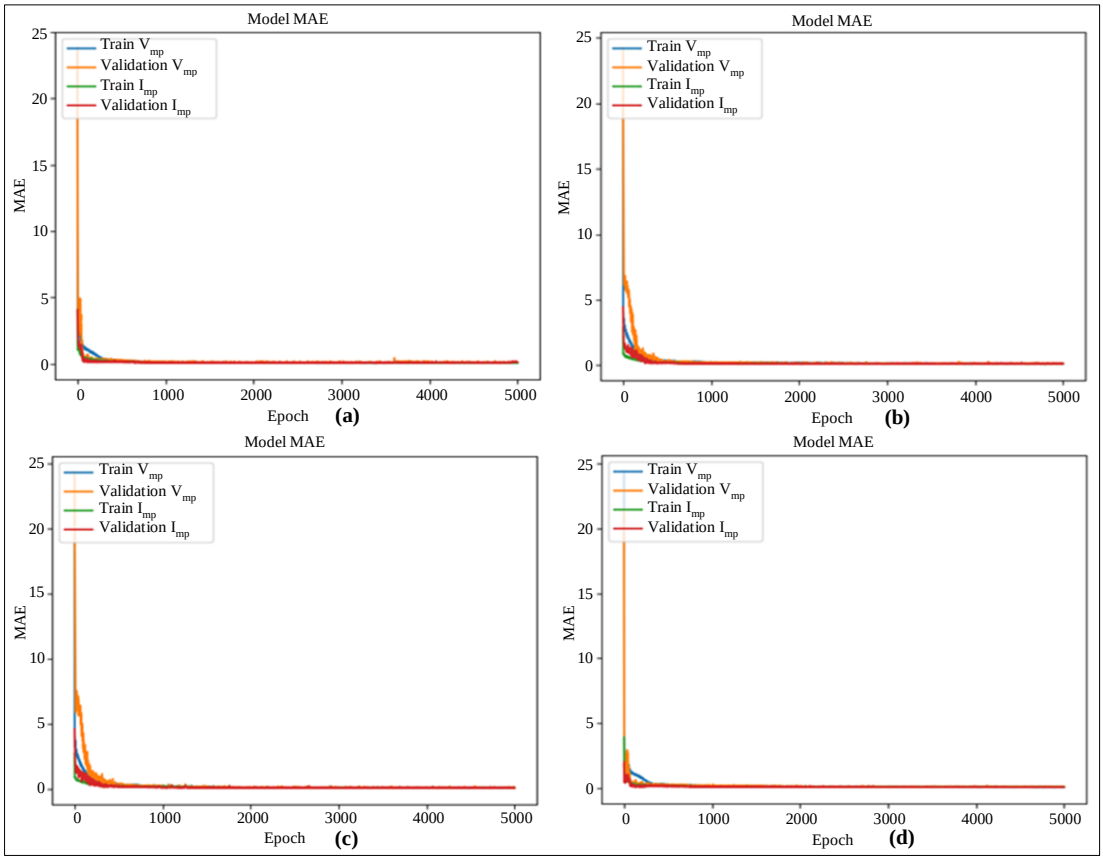

Fig. 8 Comparison of model MAE across epochs for (a) GRU, (b) CNN, (c) GRU-CNN, and (d) CNN-GRU architectures.

Four subfigures in Figure 8 show how Epochs and MAE relate to the GRU, CNN, GRU-CNN, and CNN-GRU models. Four curves representing training and validation MAE for both Vmp and Imp are shown in each subfigure. The GRU model is shown in Figure 8(a) with a consistent drop in MAE for both training and validation sets, showing strong generalization but with a slightly larger validation MAE, particularly for Imp, reflecting middling performance.

With larger values for both training and validation sets, especially for Vmp, Figure 8(b) for the CNN model shows a less consistent decrease in MAE, indicating its reduced efficacy in capturing temporal dependencies. Because of the combined strengths of the GRU and CNN layers, the GRU-CNN model shows a more noticeable and smoother fall in MAE across all curves (Figure 8(c)).

At last, Figure 8(d) for the CNN-GRU model highlights its better performance in current prediction by displaying the most significant decrease in MAE, especially for Imp, where it obtains the lowest values. The GRU-CNN and CNN-GRU models perform better than the individual GRU and CNN models; CNN-GRU excels in Imp prediction, which is consistent with the already noted metrics.

Figure 9 gives an understanding of the predictive accuracy of the CNN-GRU model by comparing the projected values with the actual values for both Vmp and Imp. With a near alignment between the anticipated and real values, Figure 9(a) shows the model's great accuracy in predicting the maximum power point voltage.

The model's accuracy in forecasting the current at the maximum power point is seen by the prediction vs. actual Imp plot in Figure 9(b), where the projected and fundamental current values are pretty similar. As previously noted in the performance measures, the CNN-GRU model's effectiveness and superior performance in solar power prediction tasks are highlighted by this high degree of correlation in both subfigures.

Subfigures (a) and (b) of Figure 10 illustrate the correlation between residuals and frequency for Vmp and Imp, respectively, using the CNN-GRU model. The frequency at which various residual values occur is shown in Figure 10(a) by the distribution of residuals for Vmp, which also offers information about the prediction errors of the model and their dispersion around zero, therefore revealing the accuracy and possible biases in the voltage forecasts.

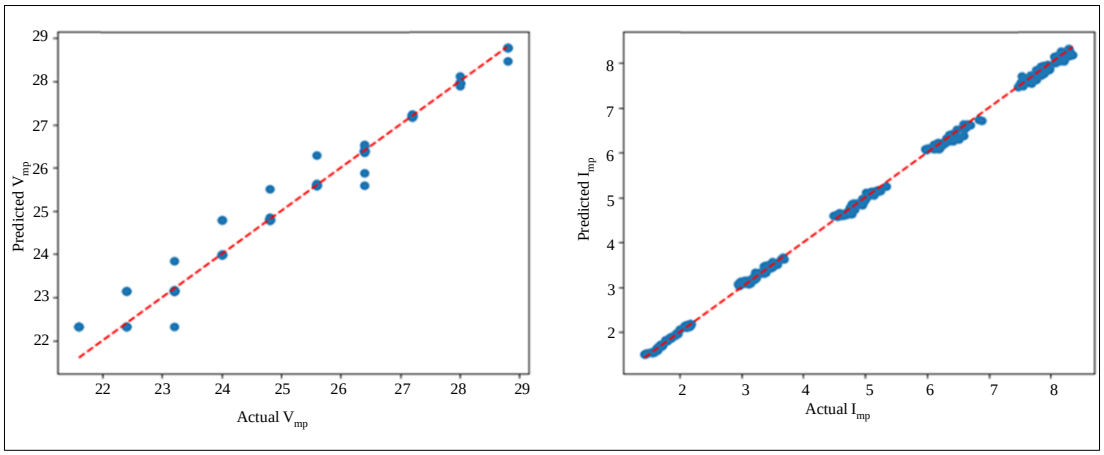

Fig. 9 Prediction vs. Actual values for (a) Vmp, and (b) Imp Using the CNN-GRU model.

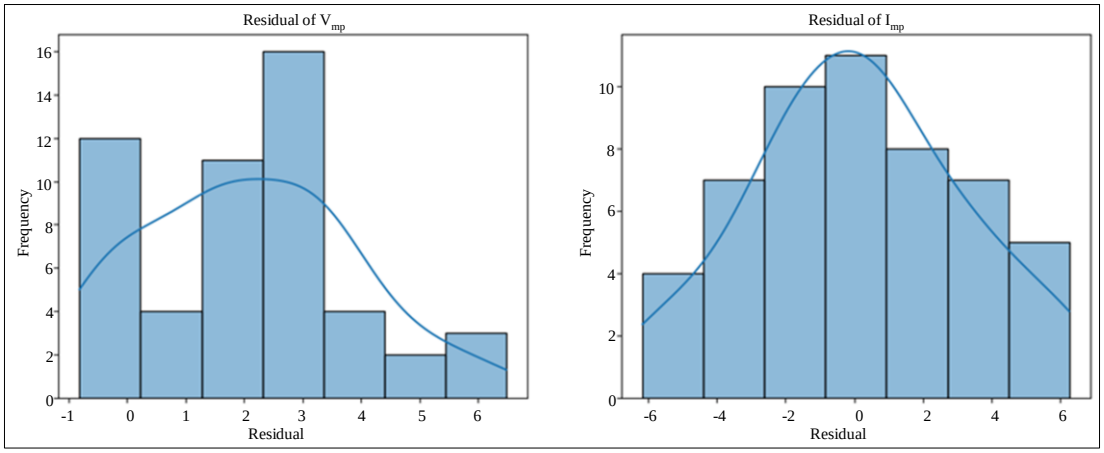

Fig. 10 Residual analysis for CNN-GRU model for (a) Vmp, and (b) Imp.

Similar residuals for Imp are shown in Figure 10(b), which emphasizes the frequency and distribution of errors in the present forecasts. Strongness in the prediction of voltage and current at the maximum power point would be demonstrated by a closely centered distribution around zero for both subfigures.

4.2. Results Analysis

As for the findings of this study, it presented a new model fusing CNN and GRU to forecast the maximum power point of solar panels. The above evaluation proves that our CNN-GRU model has a better performance compared to the other models, which could be attributed to the following aspects.

To begin with, hybrid architecture takes the best from CNN and GRU, and their combination allows us to reach our goals more quickly and with less effort. CNNs perform very well in learning spatial features of the input data to discover local representations in the irradiance and temperature.

This is to ensure that variability and intermittency of solar power data are managed in the best way possible through this spatial feature extraction. Indeed, GRUs are intended to model temporal dependencies, so a time series forecasting problem is more suitable for them. Thus, using CNNs in parallel with GRUs, the proposed model is capable of extracting high-quality spatial features and effectively learning temporal dependencies by increasing predictive accuracy.

Secondly, bidirectional GRU layers, which are incorporated into the network, also help the model capture information flow from the data. Classic GRUs work with the sequence data in a one-way manner, which can potentially leave details about relations between various time points unnoticed.

This shortcoming is handled effectively by bidirectional GRUs since the data is processed forward and backwards, which helps capture more temporal dependencies. Bidirectional to this flow, much contribution to the model meant for the identification of both Vmp and Imp is achieved.

Dropout layers and batch normalization applied to the model also reduce overfitting and provide stability for

training. Dropout layers temporarily eliminate a percentage of the neurons in a network during training to enhance the network's feature learning process. On the other hand, batch normalization normalizes the output of every layer, which has a direct impact on increasing the rate of training and the stability of the model. These techniques generally improve the ability of the model to perform well when used on data that was not used in its training, hence increasing its generality.

In regard to the performance of these models, it can be inferred that the proposed CNN-GRU model outperforms the stand-alone GRU and CNN models for the specific task. Although the stand-alone GRU model is sensitive to temporal dependencies, it is incapable of learning spatial features that are very important to solar power forecasting. The stand-alone CNN model is adept at spatial feature extraction but is inadequate when it comes to temporal modeling.

5. Conclusion

A thorough investigation of forecasting MPP in solar panels using a variety of neural network architectures: GRU, CNN, GRU-CNN, and CNN-GRU models is presented in this article. It is clear from thorough testing and assessment that the hybrid models-more significantly, GRU-CNN and CNN-GRU outperform individual GRU and CNN models in terms of accuracy measures like MAE, MSE, and coefficient of determination (R^2). While the CNN-GRU model shines especially at current prediction, the GRU-CNN model strikes a delicate balance between precise voltage (Vmp) and current (Imp) predictions. Furthermore, confirming the correctness and robustness of the CNN-GRU model is a residual analysis. These results highlight how well convolutional and recurrent layers combined to capture temporal and spatial patterns, respectively, to improve solar energy forecasting prediction performance. Through its insights into the use of sophisticated neural network architectures to enhance MPP prediction in solar panels, the work advances the area of renewable energy.

Future studies might enhance prediction performance even more by investigating more hybrid designs or adding attention techniques. Real-time data streams and outside variables like weather forecasts could also improve the robustness and application of the models in real-world solar energy systems. Evaluation of the model's performance in different environmental settings and scaling up to more enormous datasets for broader applicability and validation could be the main topics of future study.

Funding Statement

This study was performed with the support of Jamhuriya University of Science and Technology, Mogadishu, Somalia.

Availability of Data and Materials

The data are available online as in reference [32].

Acknowledgments

The authors would like to extend their gratitude to the engineering faculty of Jamhuriya University of Science and Technology for their invaluable assistance and support throughout this research. Special thanks are due to the Department of Electrical Engineering for their guidance and contributions. The authors also appreciate the cooperation and encouragement from their colleagues and peers.

References

[1] Gangqiang Li et al., "Photovoltaic Power Forecasting with a Hybrid Deep Learning Approach," *IEEE Access*, vol. 8, pp. 175871-175880, 2020. [CrossRef] [Google Scholar] [Publisher Link]

[2] Banalaxmi Brahma, and Rajesh Wadhvani, "Solar Irradiance Forecasting Based on Deep Learning Methodologies and Multi-Site Data," *Symmetry*, vol. 12, no. 11, pp. 1-20, 2020. [CrossRef] [Google Scholar] [Publisher Link]

[3] Pantelis Capros, Nikolaos Tasios, and Adamantios Marinakis, "Very High Penetration of Renewable Energy Sources to the European Electricity System in the Context of Model-Based Analysis of an Energy Roadmap towards a Low Carbon EU Economy by 2050," *2012 9th International Conference on the European Energy Market*, Florence, Italy, pp. 1-8, 2012. [CrossRef] [Google Scholar] [Publisher Link]

[4] Imran Pervez et al., "Most Valuable Player Algorithm Based Maximum Power Point Tracking for a Partially Shaded PV Generation System," *IEEE Transactions on Sustainable Energy*, vol. 12, no. 4, pp. 1876-1890, 2021. [CrossRef] [Google Scholar] [Publisher Link]

[5] J.C. Hernandez, O.G. Garcia, and F. Jurado, "Photovoltaic Devices under Partial Shading Conditions," *International Review on Modelling and Simulations*, vol. 5, no. 1, pp. 414-425, 2012. [Google Scholar]

[6] Premkumar Manoharan et al., "Improved Perturb and Observation Maximum Power Point Tracking Technique for Solar Photovoltaic Power Generation Systems," *IEEE Systems Journal*, vol. 15, no. 2, pp. 3024-3035, 2021. [CrossRef] [Google Scholar] [Publisher Link]

[7] M.A.A. Viegas, and C.M. Affonso, "Energy Resource Management in a Smart Grid Considering Integration of Electric Vehicles and Wind Power Generation Using Simulated Annealing," *The 12th Latin-American Congress on Electricity Generation and Transmission*, pp. 1-11, 2017. [Google Scholar]

[8] Manabjyoti Daimari, and Barnali Goswami, "Firefly Based Unit Commitment," *International Journal of Engineering Research & Technology*, vol. 5, no. 12, pp. 221-225, 2016. [Google Scholar] [Publisher Link]

[9] Wenwu Li et al., "A Hybrid Forecasting Model for Short-Term Power Load Based on Sample Entropy, Two-Phase Decomposition and Whale Algorithm Optimized Support Vector Regression," *IEEE Access*, vol. 8, pp. 166907-166921, 2020. [CrossRef] [Google Scholar] [Publisher Link]

[10] Immad Shams, Saad Mekhilef, and Kok Soon Tey, "Improved-Team-Game- Optimization-Algorithm-Based Solar MPPT with Fast Convergence Speed and Fast Response to Load Variations," *IEEE Transactions on Industrial Electronics*, vol. 68, no. 8, pp. 7093-7103, 2021. [CrossRef] [Google Scholar] [Publisher Link]

[11] Mansi Joisher et al., "A Hybrid Evolutionary-Based MPPT for Photovoltaic Systems under Partial Shading Conditions," *IEEE Access*, vol. 8, pp. 38481-38492, 2020. [CrossRef] [Google Scholar] [Publisher Link]

[12] Mostefa Kermadi et al., "An Effective Hybrid Maximum Power Point Tracker of Photovoltaic Arrays for Complex Partial Shading Conditions," *IEEE Transactions on Industrial Electronics*, vol. 66, no. 9, pp. 6990-7000, 2018. [CrossRef] [Google Scholar] [Publisher Link]

[13] Saba Javed et al., "A Simple Yet Fully Adaptive PSO Algorithm for Global Peak Tracking of Photovoltaic Array under Partial Shading Conditions," *IEEE Transactions on Industrial Electronics*, vol. 69, no. 6, pp. 5922-5930, 2022. [CrossRef] [Google Scholar] [Publisher Link]

[14] Mario Tovar, Miguel Robles, and Felipe Rashid, "PV Power Prediction, Using CNN-LSTM Hybrid Neural Network Model. Case of Study: Temixco-Morelos, México," *Energies*, vol. 13, no. 24, pp. 1-15, 2020. [CrossRef] [Google Scholar] [Publisher Link]

[15] Asiye K. Ozcanli, Fatma Yaprakdal, and Mustafa Baysal, "Deep Learning Methods and Applications for Electrical Power Systems: A Comprehensive Review," *International Journal of Energy Research*, vol. 44, no. 9, pp. 7136-7157, 2020. [CrossRef] [Google Scholar] [Publisher Link]

[16] Chuang Li et al., "A Multi-Energy Load Forecasting Method Based on Parallel Architecture CNN-GRU and Transfer Learning for Data Deficient Integrated Energy Systems," *Energy*, vol. 259, 2022. [CrossRef] [Google Scholar] [Publisher Link]

[17] Guangxu Chen et al., "Time Series Forecasting of Oil Production in Enhanced Oil Recovery System Based on a Novel CNN-GRU Neural Network," *Geoenergy Science and Engineering*, vol. 233, 2024. [CrossRef] [Google Scholar] [Publisher Link]

[18] T. Sana Amreen, Radharani Panigrahi, and Nita R. Patne, "Solar Power Forecasting Using Deep Learning Approach," *International Symposium on Sustainable Energy and Technological Advancements*, pp. 83-93, 2023. [CrossRef] [Google Scholar] [Publisher Link]

[19] Qing Li et al., "A Multi-Step Ahead Photovoltaic Power Forecasting Model Based on TimeGAN, Soft DTW-Based K-Medoids Clustering, and a CNN-GRU Hybrid Neural Network," *Energy Reports*, vol. 8, pp. 10346-10362, 2022. [CrossRef] [Google Scholar] [Publisher Link]

[20] Abdellatif Ait Mansour, Amine Tilioua, and Mohammed Touzani, "Bi-LSTM, GRU and 1D-CNN Models for Short-Term Photovoltaic Panel Efficiency Forecasting Case Amorphous Silicon Grid-Connected PV System," *Results in Engineering*, vol. 21, pp. 1-10, 2024. [CrossRef] [Google Scholar] [Publisher Link]

[21] Amit Rai, Ashish Shrivastava, and Kartick C. Jana, "Differential Attention Net: Multi-Directed Differential Attention Based Hybrid Deep Learning Model for Solar Power Forecasting," *Energy*, vol. 263, 2023. [CrossRef] [Google Scholar] [Publisher Link]

[22] Yaojian Xu et al., "A Complementary Fused Method Using GRU and XGBoost Models for Long-Term Solar Energy Hourly Forecasting," *Expert Systems with Applications*, vol. 254, 2024. [CrossRef] [Google Scholar] [Publisher Link]

[23] Shyam Singh Chandel et al., "Review of Deep Learning Techniques for Power Generation Prediction of Industrial Solar Photovoltaic Plants," *Solar Compass*, vol. 8, pp. 1-12, 2023. [CrossRef] [Google Scholar] [Publisher Link]

[24] A. Mellit, A.M. Pavan, and V. Lughi, "Deep Learning Neural Networks for Short-Term Photovoltaic Power Forecasting," *Renewable Energy*, vol. 172, pp. 276-288, 2021. [CrossRef] [Google Scholar] [Publisher Link]

[25] Pengtao Li et al., "A Hybrid Deep Learning Model for Short-Term PV Power Forecasting," *Applied Energy*, vol. 259, 2020. [CrossRef] [Google Scholar] [Publisher Link]

[26] Hanxun Zhou et al., "An Android Malware Detection Approach Based on SIMGRU," *IEEE Access*, vol. 8, pp. 148404-148410, 2020. [CrossRef] [Google Scholar] [Publisher Link]

[27] Md. Jalal Uddin Chowdhury et al., "Plant Leaf Disease Detection and Classification Using Deep Learning: A Review and A Proposed System on Bangladesh's Perspective," *International Journal of Science and Business*, vol. 28, no. 1, pp. 193-204, 2023. [CrossRef] [Google Scholar] [Publisher Link]

[28] Suleiman Y. Yerima et al., "Deep Learning Techniques for Android Botnet Detection," *Electronics*, vol. 10, no. 4, pp. 1-17, 2021. [CrossRef] [Google Scholar] [Publisher Link]

[29] Yinhong Tian et al., "A Novel Deep Learning Method Based on 2-D CNNs and GRUs for Permeability Prediction of Tight Sandstone," *Geoenergy Science and Engineering*, vol. 238, 2024. [CrossRef] [Google Scholar] [Publisher Link]

[30] Shahzeb Khan, and Vipin Kumar, "A Novel Hybrid GRU-CNN and Residual Bias (RB) Based RB-GRU-CNN Models for Prediction of PTB Diagnostic ECG Time Series Data," *Biomedical Signal Processing and Control*, vol. 94, 2024. [CrossRef] [Google Scholar] [Publisher Link]

[31] Mohammad G. Zamani et al., "Hybrid WT-CNN-GRU-Based Model for the Estimation of Reservoir Water Quality Variables Considering Spatio-Temporal Features," *Journal of Environmental Management*, vol. 358, 2024. [CrossRef] [Google Scholar] [Publisher Link]

[32] Ruhi Sharmin, Dataset for MPPT Model, Harvard Dataverse, 2022. [Online]. Available: https://dataverse.harvard.edu/dataset.xhtml?persistentId=doi:10.7910/DVN/IH6AC2